Engineering and Technology Journal

Thermal Performance of an Evacuated-Tube Solar Collector Using Nanofluids and an Electrical Curtain Controlled by an Artificial Intelligence Technique

Hussam J. Rashid*, Khalid F. Sultan, Hosham S. Anead

Electromechanically Engineering Dept., University of Technology-Iraq, Alsina'a Street, P.O Box 10066, Baghdad, Iraq.
*Corresponding author Email: eme.19.19@grad.uotechnology.edu

H I G H L I G H T S

- Increasing ETSC's efficiency by using Finned electronic curtain and Nano fluids .
- Using of finned electronic curtain increased sun rays on the ETSC's that increases the system efficiency.
- Efficiency improvement with TiO2 are 7.03%, 9.16%, and 11.89%, respectively.
- using artificial intelligent (FLC–ANN) to predict the thermal parameters of ETSCs.

A R T I C L E   I N F O

A B S T R A C T

This paper studies the improvement of an evacuated tube solar collectors(ETSCs) performance in two way. The first is by adding a finned electronic curtain in front of the solar collector. While the second is by using a nanofluid instead of pure water. The purpose of the curtain is to increase the amount of solar radiation reflected toward the collector. The curtain is distinguished by its self-ability to track the sun's rays automatically. The electronic curtain is also closed to shade the tubes depending on the movement of the electronic curtain's fins and the nanofluid's temperatures. MATLAB algorithm has been used to design the Simulink model and control the system using Fuzzy Logic Control (FLC) and Artificial Neural Network (ANN). The results showed that the system performance improved using TiO2(50nm)+PW) as a working fluid without the curtain are (3.906%,5.34%, and7.407%), while the rate of improvement in the case of distilled water only was 2.34% and3.81%. Finally, by adding the finned electronic curtain to the system and use of $TiO_2(50nm)+PW$ as a working fluid, the efficiency increased by 7.03%,9.16%, and 11.89%. The results showed that the performance of evacuated tubes solar collectors increased by using a nanofluid and the finned electronic curtain.

1. Introduction

Solar energy is a significant source of renewable energy that can be used with various techniques. Photovoltaic (P.V.) modules transform sunlight into electricity, while the heat collectors harvest the heat energy. However, to make this technology a primary source for the future, many problems need to be addressed such as efficiency, storage, and environmental effects including dust, temperature, and moisture [1]. Solar energy is the cleanest, inexhaustible energy, and cheap compared to other types of renewable energies. Solar power is now becoming a wide field used because it's safe and can also be accessed without constraints. In order to collect heat from solar power, solar collectors are the current technologies that can be used for many of the energy consumption of buildings, such as air conditioning, water heating, heating of swimming pools, and so on [2]. Performance of the solar power systems improved through various methods including the nanofluid as a working fluid. Nanofluids are the most appealing way to improve the performance of heat transfer systems because of the high thermal conductivity, and many forms of the nanoparticles have been presented. Metal and metal-oxide nanoparticles with a diameter of less than 100nm are added to the base fluid to produce it. Renewable energy makes the use of the nanofluids special in the solar collectors. Nanofluids improved the working fluid's heat transfer coefficient by increasing its thermal conductivity and allowing it to transport large quantities of the thermal energy by increasing its density and specific heat product. [3]. Many researchers such as Omer Khalil et al. were interested in evacuated tube solar collectors [4]. This study presents a mathematical model to investigate the performance of a photovoltaic/thermal collector with upper and lower reflectors and a glass cover by using a nanofluid (AL_2O_3-H_2O). The average daily thermal efficiency by the two reflectors without nanofluid was 62.1%. In contrast, the thermal efficiency without any reflector was 59.735%. It's indicating that the reflectors have a beneficial effect on the thermal efficiency.

Figure 1: Evacuated tube solar collector

When the reflecting mirrors were presented, the electrical efficiency decreased, and the daily average of the total electrical efficiency without the reflective mirror and nanofluid was 14.6 %. Whereas, the daily average with the reflective mirror and the nanofluid was 13.67%. H. Salim Anead et al. [5] used a metal (Cu + Ag – Pw) and hybrid nanofluids (Al2O₃ + ZrO2 – Pw) as a working fluid to improve the performance of a solar hybrid nanofluid heating system and cooling it through an electronic curtain. Furthermore, hybrid nanofluid flow pressure drop and heat transfer have improved. In this study, two types of hybrid nanoparticles were employed with five-volume concentrations (1, 2, 3, 4, and 5%) and volume flow rates (20, 40, and 60 L/min) with pure water as a working fluid. Saleh Abo-Elfadl et al. [6] used the energy and exergy of integrating reflectors with an evacuated tube solar collector-heat pipe (ETSC-HP) system for thermal energy storage. The results showed that the reflectors with ETSC-HP improved the input energy, storage energy, and exergy efficiency, and reduced the radiation and convection losses. Upper, lower, and both of reflectors increased the input energy to the collector by roughly 15.3%, 22.5%, and 37%, respectively. Moreover, it increased the output daily storage energy by 14%, 22.1%, and 35.7%, respectively compared to the system without reflectors. Another study looks into nanofluids made of artificial materials, and the results showed that its improved ETC performance [7]. Many authors have stated that the ETSCs increased the efficiencies compared with the frequent FPCs, especially at low temperatures and insulation [9]. An ETC made of equivalent evacuated glass tubes. All evacuated pipes including two tubes, internal and external tubes. The inner tube is coated with a careful layer, but the outside pipe is clear. Rays of light carry out across the clear outer tube and absorbed toward the inner tube. Each internal and external tubes own the least reflective characteristics. The inside tube heats up as the sunlight across through the outside pipe and keeps the inside tube's heat, as shown in Figure 1.

2. Material

The dimensions of the evacuated tube solar collector curtain with fins are 160 x 86 cm which are made from aluminum. The frame is made of aluminum sheets with dimensions of 10 cm of width and a height of 5 cm. The fins are also made of aluminum with dimensions of 10 cm in width and 1 cm in thickness or height. The number of fins are 13 fins. Inside the fins, reflective mirrors have used to reflect the sun. The inner surface contains on the fins as shown in Figure 2.

2.1 Mirror

A mirror is an object that reflects an image. The light that bounces off a mirror will show an image of whatever is in front of it when focused through the lens of the eye or a camera. Mirrors reverse the direction of the image in an equal yet opposite angle from which the light shines upon it. This helps the spectator to see themselves or objects behind them as well as objects that are in their field of vision but are at an angle from them such as around a corner. Natural mirrors have been around since the dawn of time. Such as the surface of the water, people have been manufacturing mirrors out of a variety of materials for thousands of years like stone, metals, and glass. Metals such as silver or aluminum are often used in modern mirrors due to their high reflectivity and are applied as a thin coating on the glass due to its naturally smooth and hard surface.

A wave reflector is a mirror. Light is made up of waves, and when those waves bounce off the flat surface of a mirror, they maintain the same degree of curvature and convergence as the initial waves but in the opposite direction. Light can also be visualized as rays (imaginary lines radiating from the light source that are always perpendicular to the waves). These rays are reflected at an equal yet opposite angle from which they strike the mirror (incident light). This property is called specular reflection.

2.2 Reflectivity of mirror

The proportion of reflected light is divided by the total amount of incident light that determines a mirror's reflectivity. The reflectivity will change depending on the wavelength. The mirror absorbs all or a part of the light that is not mirrored although some of it can still pass through. Despite the fact that the coating can absorb a small amount of light, the reflectivity is usually higher for first-surface mirrors, eliminating both reflection and absorption losses from the substrate. The reflectivity is often determined by the type and thickness of the coating. When the coating thickness is sufficient to prevent transmission, all of the losses occur due to absorption. Aluminum is harder, less expensive, and more resistant to tarnishing than silver which reflects about 85 to 90% of the light in the visible to the near-ultraviolet range but experiences a drop in its reflectance between 800 and 900 nm.

Figure 2: Fins of Evacuated tubes

2.3 Plane mirror

It is a plain sheet of glass and is the most common type of mirror, one of its surfaces is covered with a reflective material. The characteristics of the image in the plane mirror:

A plane mirror always forms a virtual image. A virtual image is produced when the light rays from a source that does not cross or meet a point to form an image.

The image formed or produced by a plane mirror is always of the same size as that of the object.

The distance between the object and the mirror is equal to the distance between the mirror and the image. Besides, the image formed is also erect.

Another exclusive characteristic of the image formed by a plane mirror states that the image is inverted.

2.4 Uses of a plane mirror

- Looking glass.
- Solar cookers.
- Constructing periscope, which is used in submarines
- Various scientific instruments [10-12].

3. Experimental Setup

3.1 Linear Actuator LAD 500N 15mm/s 12V - 15cm stroke

A powerful electric drive with a protection glass of IP65 and a maximum extension of 15 cm is suitable for a supply voltage of 12V. The device allows to increase the force up to 50 kg (500 N) and works with a speed of 15 mm/sec. The power consumption of the drive is not more than 2A. The electronic circuit of control is Arduino R3. The operation mechanism of the linear actuator used to move the fins of the electronic curtain upward and downward according to the time that the Arduino card programmed as well as to follow the solar rays that give the system automatically tracking to sun move during the day.

3.2 DS1302 Real Time Clock RTC Module

An electronic clock model (seconds, minutes, hours) with a calendar (days, weeks, months, years) up to the year 2100 with the leap years feature can be connected with any controller such as the Arduino via the I2C protocol and benefit from it with many time-related applications such as turning on and off at times specific data or recording complete data within a specified period of time with data times and dates.

This time is linked to the Arduino so that the opening and tracking of the feathers to the sun's rays become in time and do not need to connect the calculator to the program of the Arduino. It opens automatically after programming, as shown in Figure 3.

3.3 BLE Bluetooth 4.0:

This is compatible with iOS (iPhone) and Android devices. This device connects to the Arduino and is used to connect the phone to the Arduino for control of the evacuated tube system.

3.3.1 Two Channels Relay 5V Module with Optocoupler

- Relay contact capacity 250V and 10A. Relay output normally open, normally closed;
- Active low. 5V relay signal input voltage range:0-5V.

The VCC system power. JD-VCC relay power. Default 5V relay. JD-VCC and VCC shorted. Relay contact capacity of 250V and 10A. Relay output normally open, normally closed; Low level valid.

When the application opens in the smartphone, it will ask the user to connect to the system via the BlueTooth device. The interface is shown in Figure 3 . When the system opens via the application, the system moves the curtain according to the time, which means if the time was 10 am, the curtain will move according to the distance that set for 10 am as well as giving the ability to move the fins of the curtain one step up or down when it needs to control it manually like manual remote control. The smartphone application is an auxiliary part of the system that helps the user to work on the system more easily. Also, it keeps pace with the development of modern information and communication technology. The mechanism of controlling the finned curtain via smartphone is shown in Figure 3.
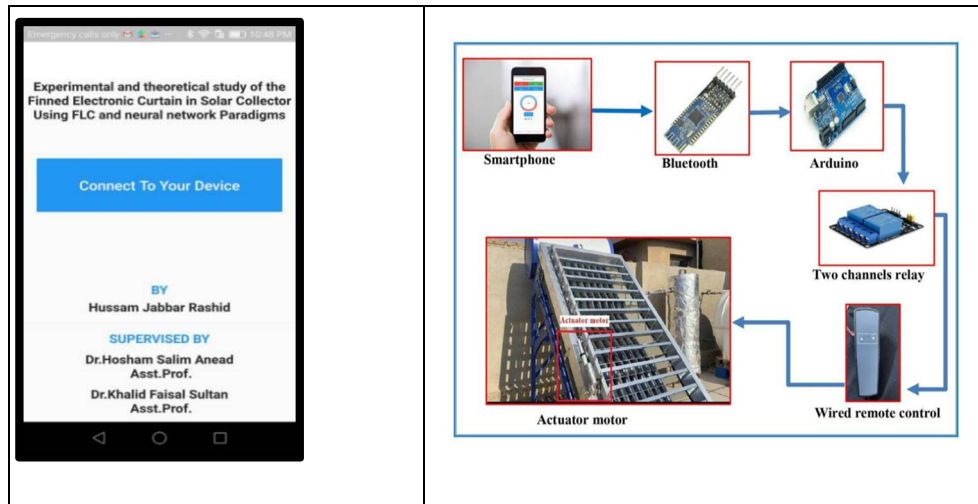
Figure 3: echanism of controlling the finned curtain via smartphone

4. Preparing of Nanofluids

To prepare the nanofluid, TiO2(50nm) was added to pure water. The blends were independently steered then further homogenized via sonication at 100 kHz, 300 W at 25 – 30 oC for two hours to ensure any aggregates' dissociation. The resulting fluids of the weight percent nanofluid were 15 – 35 wt %. These mixe with pure water using a sum of devices such as the density of the nanofluid, measurement of dynamic viscosity, thermal measurement conductivity, and measurement of specific heat as shown as in Figure 4. The properties of nanofluid can be seen in Table 1.

Figure 4: Nanofluid for TiO_2(50nm))and Pure Water

Table 1: Specifications of Nanofluid

Base fluid	Pr	ρ (Kg/m³)	Cp (J/kg k)	k (W/m k)	β *10⁵ (k⁻¹)	α*10⁵ (m²/s)
Water	6.2	997.1	4179	0.613	21	
Titanium Oxide (TiO₂)		4250	686.2	8.953	0.9	0.31

4.1 Physical Properties of the NanoFluid

The thermal properties of the working fluids are changed due to the influence of the nano properties depending on the concentration of nanoparticles and fluid temperature.

The nanofluid volume concentration is defined as [13-14]:

$$\mu_{nf} = (1 + 2.5\emptyset)\mu_f \tag{1}$$

The viscosity is calculated by [8]:

$$\mu_{nf} = (1 + 2.5\emptyset)\mu_f \tag{2}$$

The thermal conductivity of the Nanofluid mixture is derived by Maxwell for spherical particles [15-16]:

$$K_{nf} = \left(\frac{k_p + 2k_f + 2(k_f - k_p)\emptyset}{k_f + 2k_f - 2(k_f - k_p)\emptyset}\right) \tag{3}$$

The Nanofluid density for all volume concentrations is [17]

$$\rho_{nf} = (1 - \emptyset)\rho_f + \emptyset\rho_p \tag{4}$$

The specific heat of Nanofluid is calculated from this equation for all volume concentrations [13]:

$$(c_p)_{nf} = (1 - \emptyset)(c_p)_f + \emptyset(c_p)_p \tag{5}$$

5. Experimental Procedure

In this research, the performance of ETSCs was assessed and improved using nanofluids. The experiment was carried out utilizing three different volumes and concentrations for nanoparticles of 1% 3%, and 5%. The solar collector's thermal performance was tested at different mass flow rates of 15,30 and 45 Lpm. To supply the system with nanofluids, the nanoparticles were mixed with distilled water, then the required amount of nanofluid and water as a working fluid was pumped through the loop. On another hand, the global valve was used to control the flow rate on the shell and coil sides. Furthermore, the nanofluids were tested under two conditions: first without using an electronic finned curtain, and second with apply an electronic finned curtain. The flow rate is controlled by the pump speed contains three speeds to achieve the desired flow rate.

6. Artificial Intelligent Technique

6.1 Fuzzy Logic Control Systems

Zadeh was the first person to develop the fuzzy logic (1965) based on the fuzzy sets. The fuzzy set theory provides a means for representing uncertainty. In general, probability theory is the primary tool for analyzing uncertainty and assumes that uncertainty is a random process. However, not all uncertainty is random, and fuzzy set theory is used to model uncertainty associated with imprecision, vagueness, and lack of information. The following is a block diagram of a fuzzy control system as shown in Figure 5. The fuzzy controller is composed of the four components mentioned below [19-20]. To run a Simulink model of control, and fins distance open from 45 to 90 at the time from 8:30 to 12 AM and decrease from 85 to 45 at time 13 to 16:30 PM in MATLB\Simulink 2019 by inter inputs and outputs (time and distance) to fuzzy logic. Then, write rules as a membership function of input and output. After filling a requirement in the toolbox of fuzzy logic, export all data build in Matlab to the Simulink model. Figures 6, 7, and 8 show respectively the input of FLC, rules of FLC, and Simulink model of FLC.

6.2 Artificial neural networks Technique (ANNs)

Artificial Neural Networks Technique (ANNs) attempts to emulate their biological counterparts. A simple model of a neuron was proposed in 1943 by McCulloch and Pitts. Artificial Neural Network Technique (ANN) is a mathematical model that tries to simulate the structure and functionalities of biological Neural Networks. Every artificial neural network's basic building block is an artificial neuron that is a simple mathematical model (function). The model has three simple sets of rules: multiplication, summation, and activation inputs. Artificial neurons are weighted at the entrance, meaning that every input value is multiplied by the individual weight. The sum function which adds all weighted inputs and biases is the artificial neuron's middle section. The sum of previously weighted inputs and bias passes through the activation mechanism known as the transfer function as the artificial neuron exits [18]. Figure 9 shows the Simulink model of ANN. ANN is used here to control the evacuated tube by run a Simulink model of control and opens fins from distance from 45 to 90 at the time from 8:30 to 12 AM and decreases from 85 to 45 at time 1 to 4:30 PM in MATLB\Simulink 2019 by inter inputs and outputs (time and distance) to Artificial Neural Network (ANN) in code write in m_file and create a block of ANN. Finally, it can export the block of ANN in Matlab to the Simulink model. Figures 10, 11, and 12 show respectively, the Simulink model of ANN, training of ANN, and the distance in Artificial intelligent technique.
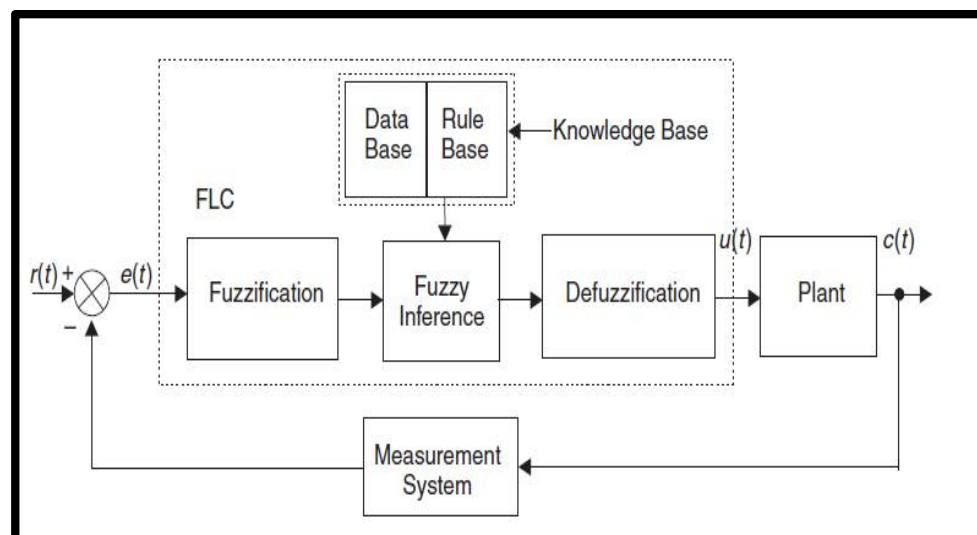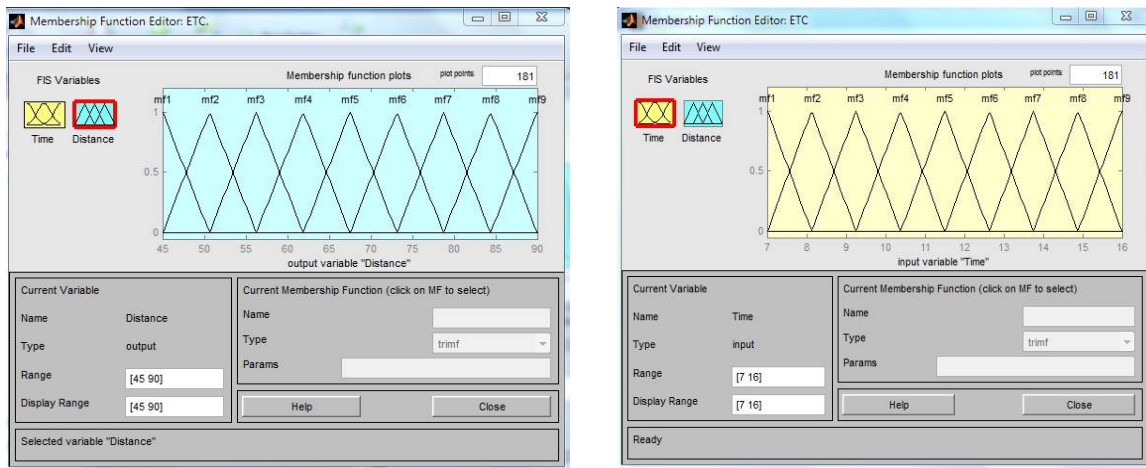

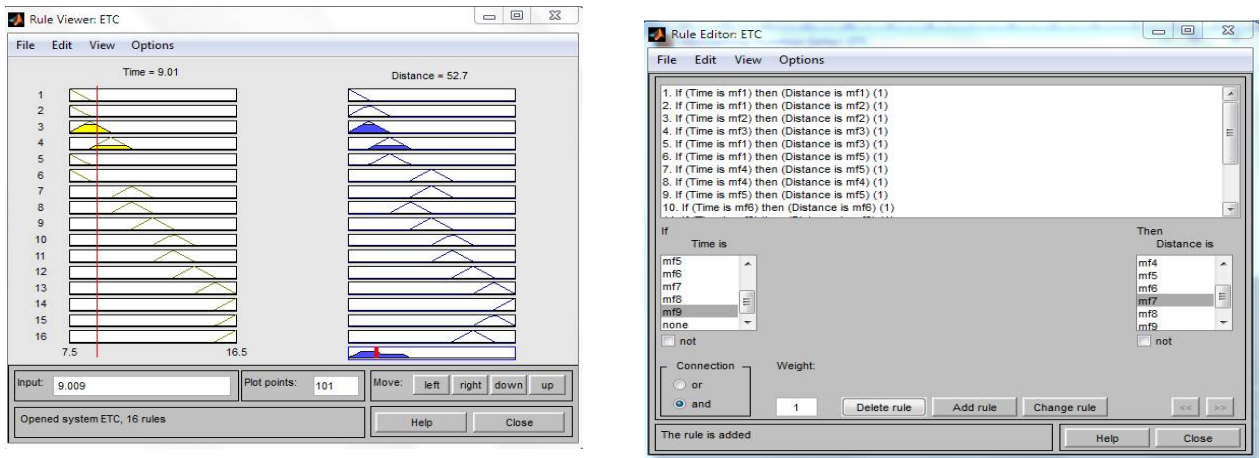**Figure 5:** Structure of FLC [19]

Figure 6: Inputs of FLC
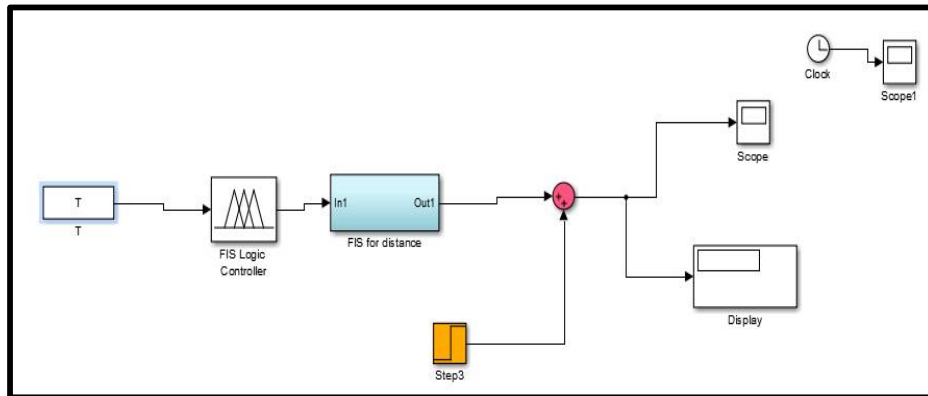

Figure 7: Rules of FLC

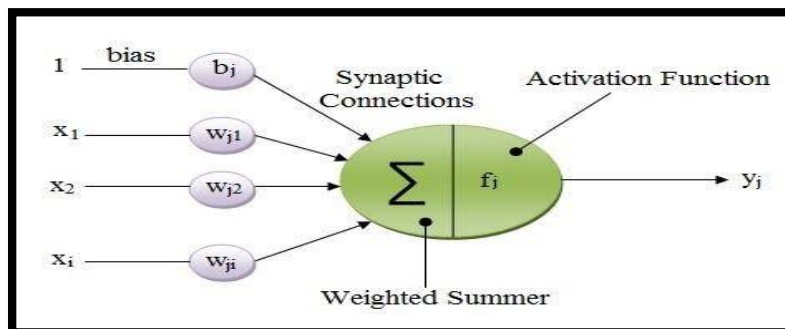**Figure 8:** Simulink model of FLC

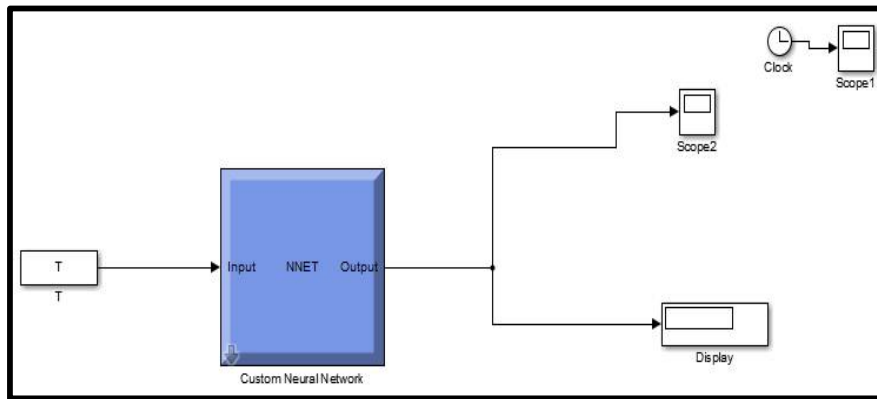**Figure 9:** Structure of neural network [12]

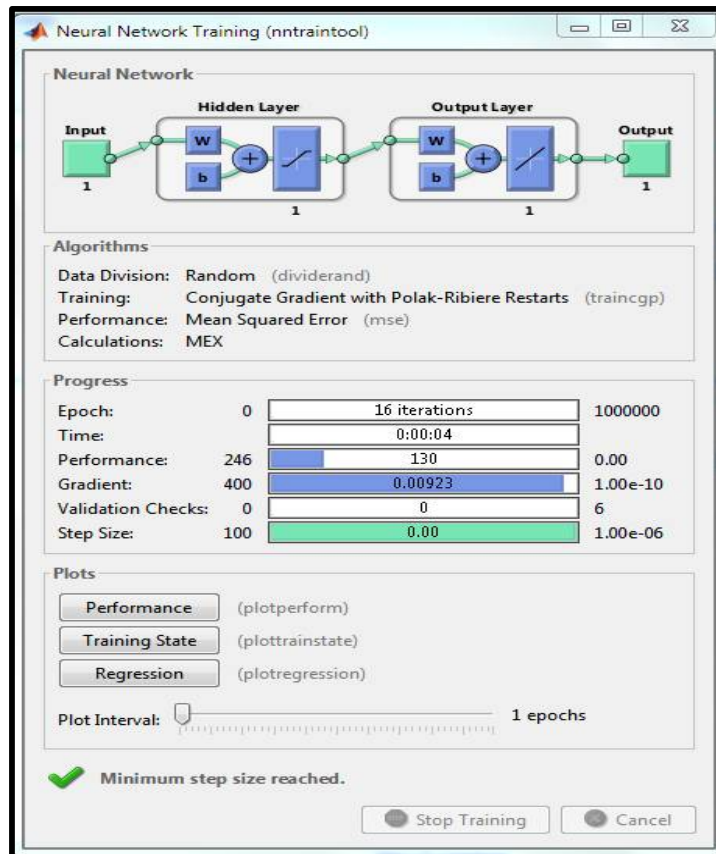**Figure 10:** Simulink model of ANN
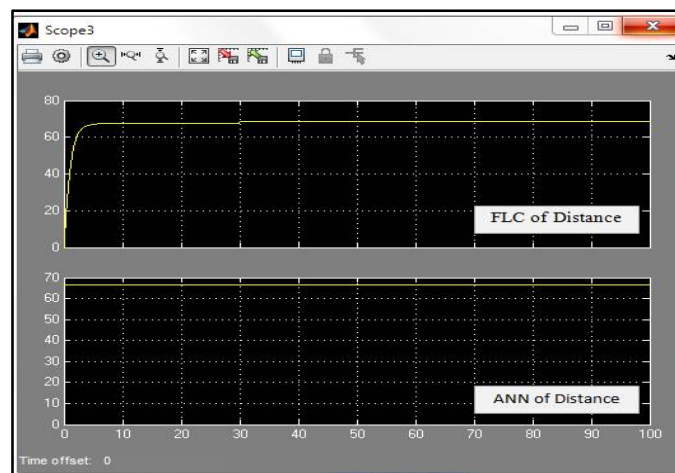

Figure 11: Training of ANN

Figure 12: distance in Artificial telligent technique

7. Results of The Experimental Work

7.1 Results of Solar collector without Fins

Firstly, Figure 13 illustrated using of the TiO_2(50nm)+PW) nanofluids at concentrations of 1, 3, and 5 vol.% with flow rates of 15, 30, and 45 Lpm, respectively. In this regard, it found that the collector efficiency is significantly increased when using nanofluids with a concentration of 5 vol%, and minimum efficiency occurs in pure water without any nanofluid.

The difference in temperature with the inlet temperature effect of concentrations and flow rates on the collector without a solar collector's fins uses pure water. These results indicated that the performance curves of a solar collector when TiO2(50nm)+PW) nanofluids are used at concentrations 1,3,5 vol% and flow rates are at 15, 30, and 45 Lpm. These curves illustrated the difference of inlet temperature (35-80°C) with the increasing of different concentrations of nanofluid and different flow rates. The maximum difference of temperature appeared in concentration and nanofluid of 5% vol, and the minimum temperature appeared in pure water without any nanofluid, as shown in Figure 14.
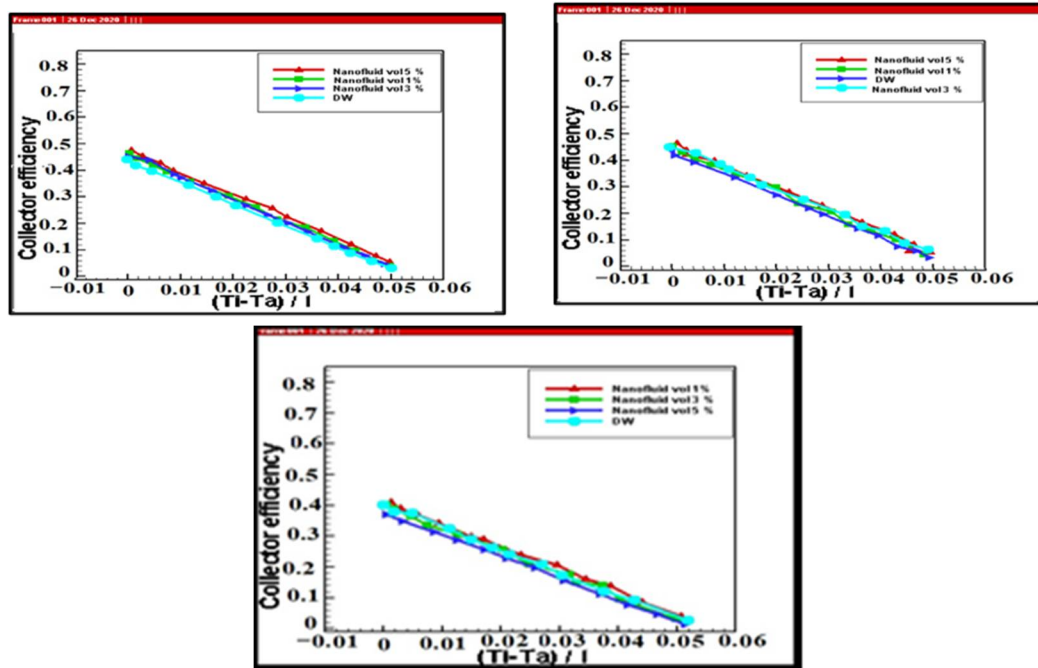

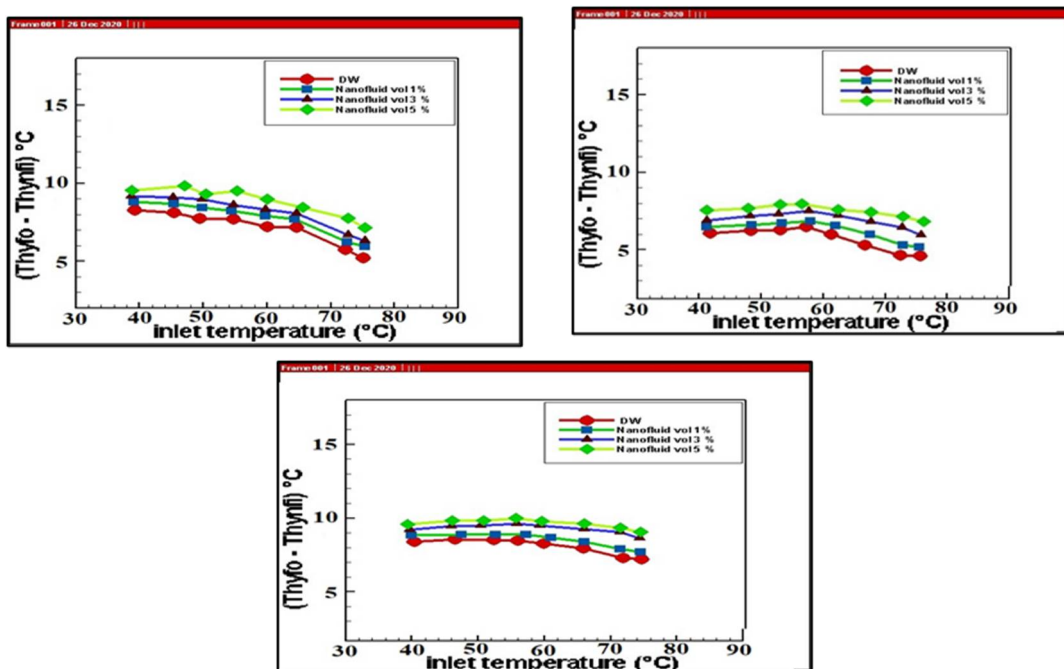**Figure 13:** Collector efficiency for φ at 15,30,45Lpm with nanofluidTiO2(50nm)+PW)

Figure 14: The difference of temperature with inlet temperature at 15,30,45Lpm with nanofluidTiO₂(50nm)+ Pure Water)

The heat transfer with inlet temperature influence of concentration of nanofluid without fins of the solar collector has been presented in this work as well as compared with using of pure water case. These results showed that the performance curves of a solar collector when TiO$_2$(50nm)+PW) nanofluids are used at concentrations (1,3 and 5 vol%), and flow rates (15, 30, and 45 Lpm). These curves illustrated the heat transfer decreased with inlet temperature increasing (35 – 80°C) in different concentrations of nanofluid and different flow rate as well as the maximum heat transfer appear in concentration an of Nanofluid (5% vol) and minimum heat transfer appeared in pure water at inlet temperature was 70 °C without any nanofluid, as shown in Figure 15.

7.2 Results of Solar collector with fins

Firstly, Figure 16 illustrates the TiO$_2$(50nm) +PW) nanofluids with fins at different flow rates (15, 30, and 45 Lpm) and concentrations (1,3 and 5 vol%). These curves observed that the efficiency of evacuated tube proportional reveres with (Ti - Ta \ I) that called φ at different nanofluid concentrations and different flow rates. So, the maximum efficiency when used concentration nanofluid of 5 vol% and minimum efficiency appeared in pure water without any nanofluid.
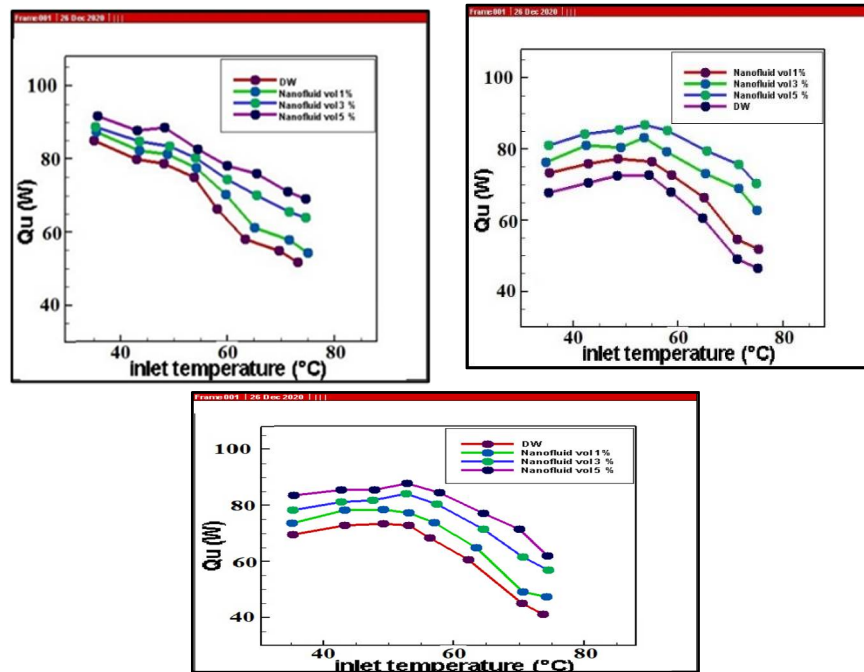
Figure 15: The heat transfer with inlet temperature at 15,30,45Lpm with nanofluid TiO$_2$(50nm)+PW)
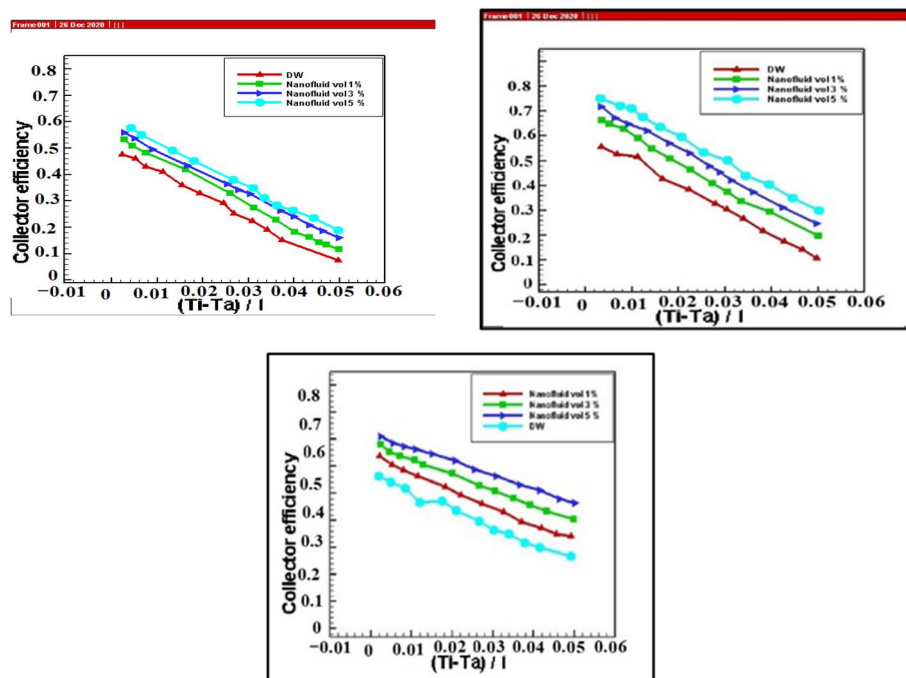
Figure 16: Collector efficiency for φ at 15,30,45Lpm with nanofluid TiO$_2$(50nm)+Pure Water

Figure 17 presents the relationship between the difference of temperature with inlet temperature effect for concentrations and flow rates on the collector with fins for a solar collector using a pure water. These results indicated that the performance curves of a solar collector when $TiO_2(50nm)+PW$ nanofluids are used at different concentrations (1,3 and 5 vol%) and flow rates (15, 30, and 45 Lpm). These curves illustrated the difference of temperature inlet temperature (35-80°C) with the increasing of different concentrations of nanofluid and different flow rates. The maximum difference of temperature appeared in the concentration of Nanofluid 5 vol%, and the minimum difference of temperature appeared in pure water without any nanofluid.

Figure 18 illustrates the relation between heat transfer with inlet temperature effect of nanofluid concentration with fins of solar collector and compared with using pure water. These results show the performance curves of a solar collector when TiO2(50nm)+PW) nanofluids are used at concentrations (1,3,5 vol%), and flow rates are (15, 30, and 45 Lpm). These curves illustrate the heat transfer decreases with inlet temperature increase (35-80°C) in different concentration of nanofluid and different flow rate as well as the maximum heat transfer appear in the concentration of Nanofluid (5 vol%) and minimum heat transfer appear in pure water at inlet temperature is 70 °C without any nanofluid.
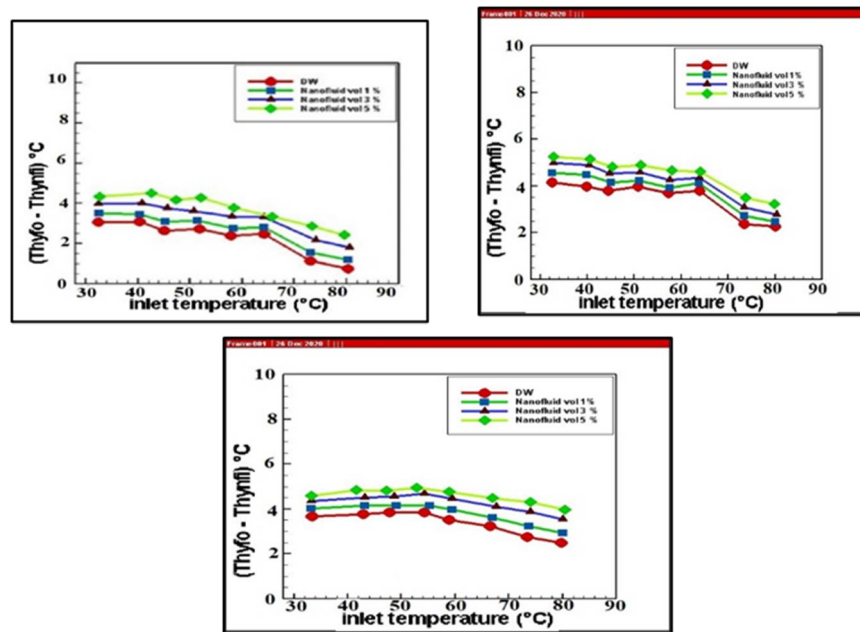

Figure 17: The difference of temperature with inlet temperature at 15,30,45Lpm with nanofluid $TiO_2(50nm)$+Pure Water)
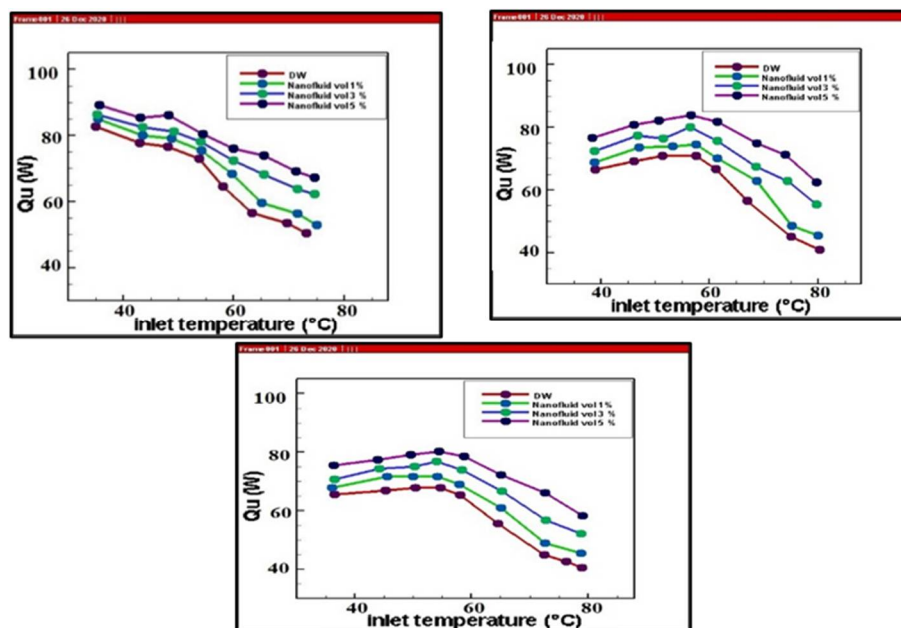

Figure 18: The heat transfer with inlet temperature at 15,30,45Lpm with nanofluidTiO2(50nm)+Pure Water)

8. Conclusions

This research introduced a theoretical and experimental study of the ETSC improvement by applying the finned electronic curtain, nanofluid as a working fluid, and artificial intelligence methods such as FLC – ANN. TiO2(50nm)+PW were used as a nanofluid due to their high thermal conductivity. Experiments were carried out using three volumes concentrations of nanofluids of 1%, 3%, and 5% vol., respectively. The thermal performance of the solar collector was examined at different flow rate volumes of 15, 30, and 45 L/min, respectively. The main outcomes of this study can be summarized as follows:

The purpose of the finned electronic curtain increased the amount of solar radiation that reflected toward the tubes to increase the efficiency of the ETSC system by programming it automatically to follow the sun's rays.

The improvement percentages using TiO_2 (50nm) + (PW) without a finned electronic curtain system were 3.906%, 5.34%, and 7.407% at three-volume concentrations of nanofluids of 1%, 3%, and 5% vol., respectively.

The obtained improvement percentages using TiO_2 (50nm) + (PW) along with utilizing the finned electronic curtain system are 7.03%, 9.16%, and 11.89% were carried out at three-volume concentrations of nanofluids of 1%, 3%, and 5% vol., respectively. These results showed that the finned electronic curtain has superior performance compared with the others due to the increment of solar radiation reflected on the evacuated Tube Solar.

The results show that the artificial intelligent method (FLC – ANN) performed well to predict the thermal parameters of the evacuated tube solar collector, besides controlling the movement of the finned electronic curtain, which is the main point for achieving the desired precision and efficiency.

The synergistic effect of the type and size of nanoparticles has an essential function in raising the heat transfer rate. The efficiency of the solar collector could be increased by the high thermal conductivity of the working fluid compared to that of distilled water.

There is a direct relationship between heat gain quantity and the concentration rates level.

Finally, as a future work, the experimental and theoretical study of the finned electronic curtain working on PV system in solar collector may be extended using artificial intelligence and an optimization of evacuated tubes solar collectors performance can be achieved by using finned electric curtain and backward flat plate reflector.

Author contribution

All authors contributed equally to this work.

Funding

Data availability statement

The data that support the findings of this study are available on request from the corresponding author.

Conflicts of interest

The authors declare that there is no conflict of interest.

References

[1] H.A. Kazem, J.H. Yousif, Comparison of prediction methods of photovoltaic power system production using a measured dataset, Energy Conv. Manag., 148 (2017)1070 –1081. https://doi.org/10.1016/j.enconman.2017.06.058

[2] M.A. Sabiha, R. Saidur , S. Mekhilef, An experimental study on Evacuated tube solar collector using Nanofluids, Trans. Sci. Technol., 2 (2015) 42 – 49.

[3] M.A. Sharafeldin , G. Grof, Evacuated tube solar collector performance using CeO2 /water Nanofluid , J. Clean. Prod., 185 (2018) 347- 356 . https://doi.org/10.1016/j.jclepro.2018.03.054

[4] A. O. Khalil, B.SH. Mohammed, The Combined Effect Of Nanofluid And Reflective Mirrors On The Performance Of Photovoltaic/Thermal Solar Collector ,Therm.Sci., 23 (2019) 573-587.

[5] H. S. Anead, Kh. F. Sultan, A. A. Hameed, Improvement the performance of solar collector (ETC) by control of polarized solar radiation and hybrid Nanofluids, (Unpublished M.A Thesis). University of Technology, Baghdad, Iraq. 2019.

[6] S . Hassan, H. El-Dosoky, Energy exergy assessment of integrating reflectors on thermal energy storage of evacuated tube solar collector-heat pipe system, Sol. Energy, 209 (2020) 470-484. https://doi.org/10.1016/j.solener.2020.09.009

[7] O. Ahmet, C. Vahit, Thermal performance of a thermosyphon heat pipe evacuated tube solar collector using silver-water nanofluid for commercial applications, Renew. Energy, 122 (2018) 26-34. http://dx.doi.org/10.1016/j.renene.2018.01.031

[8] A. Shafieian, M. Khiadani, A. Nosrati, Thermal performance of an evacuated tube heat pipe solar water heating system in cold season, Appl. Therm. Eng., 149 (2019) 644–657 .https://doi.org/10.1016/j.applthermaleng.2018.12.078

[9] K. Dick. S.Zubriski, Measurement of the efficiency of evacuated tube solar collectors under various operating conditions, College Publishing.7 (2012) 114–130. https://doi.org/10.3992/jgb.7.3.114

[10] https://www.alternative-energy-tutorials.com/solar-hot-water/solar-hot-water.html.

[11] Entry looking glass, in the online Cambridge Dictionary. Accessed on 2020-05-04

[12] Pendergrast, M. Mirror, Mirror: A History Of The Human Love Affair With Reflection,. Basic Books. 2004.

[13] M. Singh , L. Kundan, Experimental Study on Thermal Conductivity and Viscosity of Al2O3 Nano transformer Oil, Int. J. Theor. Appl. Mech. (IJTARME),. 2(2013).

[14] R. Gorla, S. Siddiqa, M. Mansour, A. Rashad , T. Salah , Heat Source/Sink Effects on a Hybrid Nanofluid-Filled Porous Cavity, J. Thermophys. Heat Transf., 31(2017). https://doi.org/10.2514/1.T5085

[15] E. Bellos, Z. Said, C. Tzivanidis, The use of nanofluids in solar concentrating technologies: a comprehensive review, J. Clean. Prod., 196 (2018) 84–99. https://doi.org/10.1016/j.jclepro.2018.06.048

[16] G. Huminic , A. Huminic, Hybrid nanofluids for heat transfer applications–A state-of-the-art review, Int. J. Heat Mass Transf., 125(2018) 82-103 . https://doi.org/10.1016/j.ijheatmasstransfer.2018.04.059

[17] I. A. Hassan, S. R. Faraj , A. K. Azeez , Theoretical temperaturedistribution investigation in electrical transformer by using nano-technology, Eng. Technol. J.,34, Part (A)(2016). http://dx.doi.org/10.30684/etj.34.12A.11

[18] X. Sui, Q. Wu, J. Liu, Q. Chen , G. Gu, A Review of Optical Neural Networks, in IEEE Access., 8(2020)70773-70783. https://doi.org/10.1109/ACCESS.2020.2987333

[19] Burns. S, Advance control engineering, Butterworth-Heinemann, Published, 2001.

[20] A. T. Nguyen, T. Taniguchi, L. Eciolaza, V. Campos, R. Palhares , M. Sugeno, Fuzzy control systems: Past, present and future, IEEE Comput. Inte. Mag., 14 (2019) 56–68. https://doi.org/10.1109/MCI.2018.2881644